



ELSEVIER

# Molecular, crystal and solution structure of a $\beta$ -cyclodextrin complex with the bromide salt of 2-(3-dimethylaminopropyl)tricyclo[3.3.1.1<sup>3,7</sup>]decan-2-ol, a potent antimicrobial drug

Anastassis Perrakis <sup>a,\*</sup>, Ekaterini Antoniadou-Vyza <sup>b</sup>, Polyxeni Tsitsa <sup>b</sup>,  
Victor S. Lamzin <sup>c</sup>, Keith S. Wilson <sup>c</sup>, Stavros J. Hamodrakas <sup>d</sup>

<sup>a</sup> *European Molecular Biology Laboratory (EMBL), c/o ILL, Av. des Martyrs, F-38042 Grenoble, France*

<sup>b</sup> *Department of Pharmacy, Division of Pharmaceutical Chemistry, University of Athens, Panepistimiopolis, GR-15771 Athens, Greece*

<sup>c</sup> *European Molecular Biology Laboratory (EMBL), c/o DESY, Notkestrasse 85, D-22603 Hamburg, Germany*

<sup>d</sup> *Department of Biology, Division of Cell Biology and Biophysics, University of Athens, Panepistimiopolis, GR-15701 Athens, Greece*

Received 23 December 1996; accepted 23 December 1998

## Abstract

The pharmacological properties of a cyclomaltoheptaose ( $\beta$ -cyclodextrin) series of adamantane-group-bearing compounds that exhibit potent antibacterial activity have been studied, both isolated and in complex with  $\beta$ -cyclodextrins ( $\beta$ CDs). In this work, the structure of the bromide salt of 2-(3-dimethylaminopropyl)tricyclo[3.3.1.1<sup>3,7</sup>]decan-2-ol (ADM-10) complexed with  $\beta$ CD and ten water molecules was studied in the solid state by X-ray crystallography and in solution by NMR spectroscopy. X-ray crystallographic studies of the complex were performed both at room and cryogenic temperatures. The long aliphatic chain of ADM-10 adopts a single conformation at low temperature in contrast to what is observed at room temperature, where two side chain conformations are seen. Both NMR and X-ray crystallography studies indicate that the adamantane moiety of ADM-10 is buried in the  $\beta$ CD cavity. Chemical shifts in NMR experiments can be explained on the basis of the crystal structure of the complex. © 1999 Elsevier Science Ltd. All rights reserved.

*Keywords:*  $\beta$ -Cyclodextrin; Antimicrobial drug; X-ray crystallography; NMR; Ab initio structure solution; Synchrotron radiation

## 1. Introduction

The properties of the torus-shaped cyclodextrin molecules (CDs), which provide a hydrophilic periphery and a hydrophobic cavity, have been described in detail [1]. CDs are well known for their ability to act as hosts to

a variety of guest molecules; this ability has been attributed to hydrogen bonding, van der Waals and polar interactions between the CD and guest molecules, release of strain energy from the cyclodextrin ring and expulsion of water molecules. Cyclodextrins are extensively used for the encapsulation of substances that are volatile, sensitive, toxic, etc. [2]. Analysis of crystal structures of cyclodextrin complexes already provided valuable insight into the

\* Corresponding author.

characterisation of the chemical nature of such interactions [3].

In the course of our investigation of the pharmacological properties of adamantane-group-bearing compounds [4] and application of cyclodextrins as drug carriers for this type of compound, the bromide salt of 2-(3-dimethylaminopropyl)tricyclo[3.3.1.1<sup>3,7</sup>]decan-2-ol (AD-M-10, Fig. 1) in complex with cyclomaltoheptaose ( $\beta$ CD), and ten water molecules was studied by means of NMR and X-ray crystallography. Quaternary ammonium antibacterials, such as ADM-10, act directly on the cell membrane of microorganisms, affecting its permeability, leading to leakage of intracellular compounds and subsequent cell death [5]. However, several micro-organisms possess impermeable outer cell membranes that prevent influx of drugs. Others lack the transport system required for entrance of the drug into the bacterial cell. In both cases, drug carriers, like CDs, may facilitate the transport through outer bacterial membranes, via aqueous channels (pores). The study of complexation characteristics of such potential drug compounds with CDs, at the molecular level, might provide a rational way of optimising their biological characteristics.

## 2. Results and discussion

*Crystal packing.*—The crystal packing is remarkably tight, with  $D_{\text{calc}} = 1.4 \text{ g cm}^{-3}$ . Ten water molecules are ‘trapped’ in the crystal lattice per molecule of the complex, each forming at least two hydrogen bonds to other atoms, including symmetry-related ones. This perhaps explains why these crystals do not dry in air and are extremely stable and well diffracting considering their size.

The equatorial plane of the cyclodextrin molecule lies at an angle of  $20^\circ$  with respect to the crystallographic  $ab$  plane. The aliphatic tail of ADM-10 extends away from the cyclodextrin in a direction almost parallel to the  $a$  axis of the cell. After the quaternary nitrogen, the direction of the chain changes by  $90^\circ$  and becomes effectively parallel to the long  $c$  axis and almost perpendicular to the equatorial plane of  $\beta$ CD. The chain gradually becomes disordered and after the C-21 atom it adopts two conformations (Fig. 2(a)). This is not observed in the low-temperature data where one of the two conformations is ‘frozen out’ (Fig. 2(b)). Towards the end of the tail, the degree of disorder is constant, as reflected in the atomic temperature factors and the distances between disordered atoms. At its end, the tail comes close to

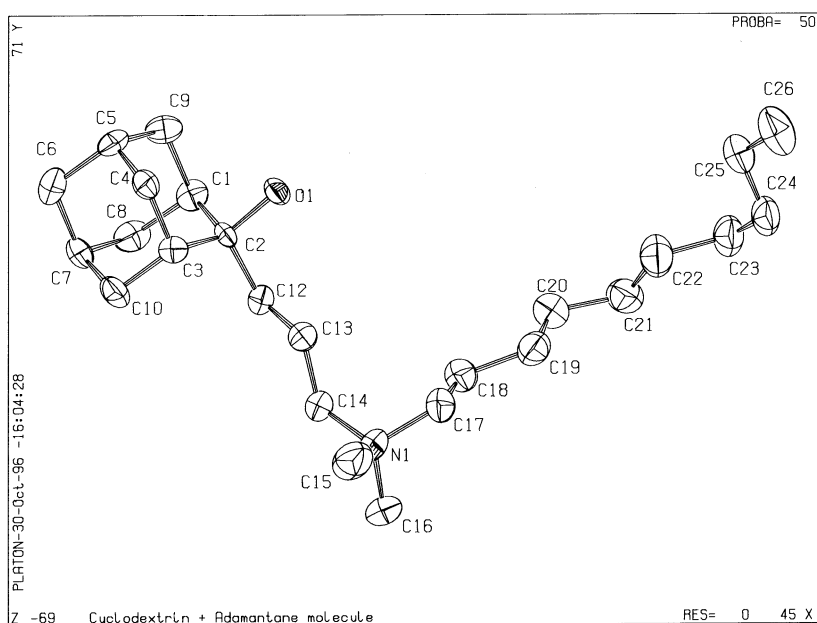


Fig. 1. The structure of the ligand, ADM-10. The 50% probability displacement ellipsoids correspond to the low-temperature structure. H atoms are excluded and all atoms are labelled. The figure was drawn by PLATON [23].

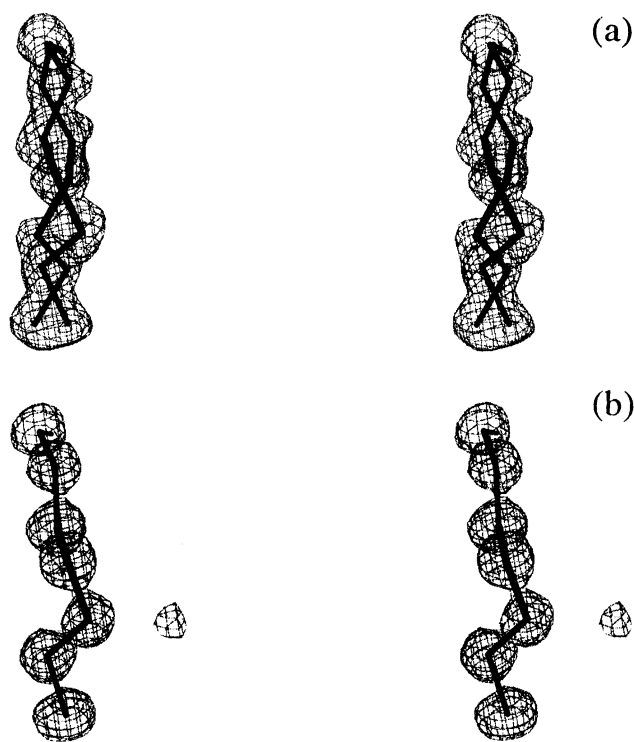


Fig. 2. Electron density maps (gray) with thick black line models, showing (a) the double conformation of the end of the methyl chain of ADM-10 at room temperature and (b) how one of these conformations is 'frozen out' at cryogenic temperature. Maps are contoured at 1 rms. The figure was drawn by O/OPLLOT [22].

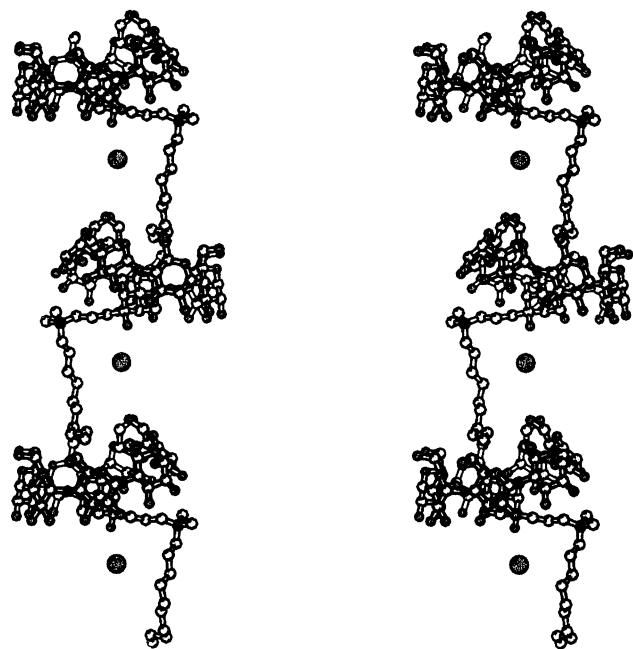


Fig. 3. A stereo view demonstrating the packing of the CD and the tails of the ADM-10 symmetry related molecules along the *c* axis. The figure was drawn by MOLSCRIPT [24].

Table 1

Close contacts of  $\beta$ CD with the bound and the symmetry related ADM-10 molecule

CD atom name	ADM-10 atom name	Distance (Å)
<i>Cyclodextrin with ADM-10 adamantane</i>		
O-4 Glc <sup>I</sup>	H-4B(4 eq)	2.68
H-3 Glc <sup>I</sup>	H-4B(4 eq)	2.43
H-3 Glc <sup>I</sup>	H-4A(4 ax)	2.33
O-4 Glc <sup>II</sup>	H-5	2.70
H-3 Glc <sup>II</sup>	H-5	2.49
H-3 Glc <sup>III</sup>	H-9A(9 eq)	2.66
H-5 Glc <sup>III</sup>	H-6B	2.67
H-3 Glc <sup>IV</sup>	H-8A	2.31
H-3 Glc <sup>IV</sup>	H-8B	2.54
H-5 Glc <sup>VI</sup>	H-10B	2.48
H-3 Glc <sup>VII</sup>	H-3	2.44

*Cyclodextrin with ADM-10 tail*

H-3 Glc <sup>V</sup>	H-12A	2.65
HO-2 Glc <sup>V</sup>	H-14A	2.10
HO-2 Glc <sup>V</sup>	H-14B	2.59
HO-3 Glc <sup>VI</sup>	H-14A	2.52

*Cyclodextrin with symmetry related ADM-10 tail*

H-6A Glc <sup>II</sup>	H-23A	2.48
H-6B Glc <sup>II</sup>	H-23A	2.57
H-5 Glc <sup>IV</sup>	H-26B	2.67

*ADM-10 adamantane with symmetry related ADM-10 tail*

H-6A (Adamantane)	H-24B	2.41
H-6B (Adamantane)	H-24B	2.66
H-7 (Adamantane)	H-26B	2.60

the molecular complex related by the  $2_1$  symmetry along *c*. It interacts both with the symmetry-related CD molecule and the adamantane moiety of ADM-10 bound to that CD (Table 1, Fig. 3). Thus, the end of the chain interacts from the opposite side of the cyclodextrin ring than that where the adamantane group lies. A large number of other symmetry contacts are formed between neighbouring molecules (data not shown).

*Description of crystal structure.*—The hydrophobic adamantane group is buried within the hydrophobic cavity of one cyclodextrin molecule (Fig. 4(a,b)). The Br<sup>-</sup> ion accepts hydrogen bonds from the O-1 atom of the adamantane moiety and three water

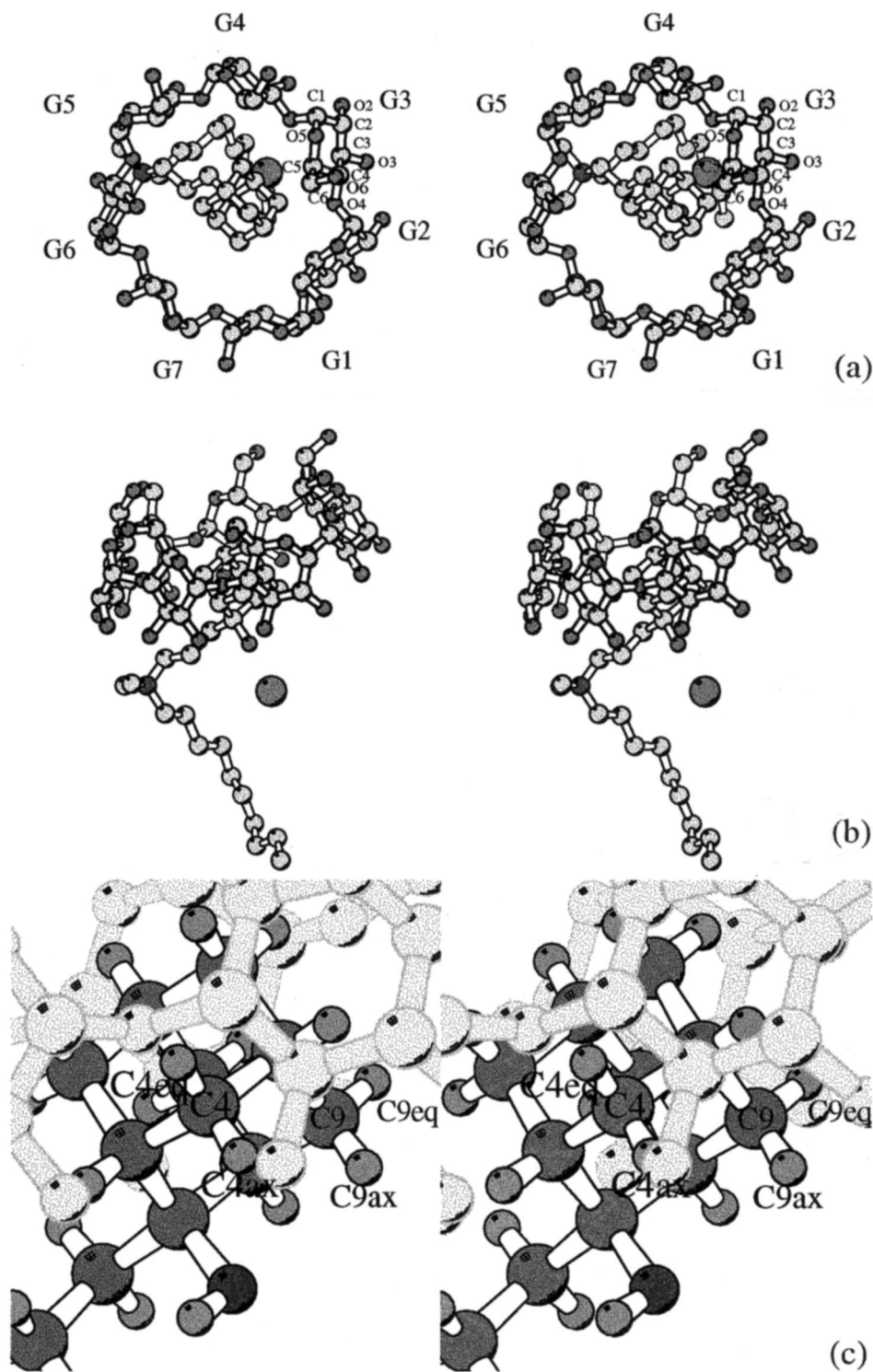


Fig. 4. Stereoscopic, ball-and-stick representations of the complex in the crystal structure. (a) Carbons are light gray and oxygens darker gray as is the nitrogen atom. The Br ion is the dark gray sphere. Hydrogen atoms are omitted. All cyclodextrin rings are numbered (G1...G7, i.e., Glc<sup>I</sup>...Glc<sup>VII</sup>). In one ring of the CD, atoms are labelled; the same labelling is used for all other rings. (b) Same as above, rotated 90° along *x*. (c) A close up of the view in the middle, including hydrogens; the important C-4 and C-9 carbons and attached hydrogens are labelled. For the adamantane, carbon atoms are dark gray, hydrogens lighter gray. The CD molecule is drawn in light gray to avoid confusion. The figure was drawn by MOLSCRIPT [24].

Table 2  
Chemical shifts (ppm) of ADM10 and  $\beta$ CD in the free and complex state

	$\delta_o$ (free)	$\delta_c$ (complex)	$\Delta\delta = (\delta_o - \delta_c)$
<i>Protons<sup>a</sup> (<sup>1</sup>H NMR in D<sub>2</sub>O)</i>			
ADM-10			
-(CH <sub>2</sub> ) <sub>9</sub> CH <sub>3</sub> (t, 3 H)	1.2768	1.2802	+0.003
-(CH <sub>2</sub> ) <sub>7</sub> - (m, 14 H)	1.3537	1.3696	+0.002
Ad (d, 2 H, 4eq, 9eq)	1.5668	1.6266	+0.071
	1.6128	1.6840	+0.071
Ad (m, 10 H)	1.7374	1.7923	+0.055
	1.7772	1.8561	+0.079
Ad (d, 2 H, 4ax, 9ax)	2.0860	2.2477	+0.162
	2.1462	2.3075	+0.163
N(CH <sub>3</sub> ) <sub>2</sub> (s, 6 H)	3.0581	3.0726	+0.014
$\beta$ CD			
H-3 ( $\times 7$ )	4.043	3.926	-0.117
	3.878	3.987	-0.102
	3.949	3.800	-0.147
H-5 ( $\times 7$ )	3.540	3.855	-0.287
	3.586	3.873	-0.315
Anomeric H ( $\times 7$ )	5.080	5.065	-0.015
	5.098	5.048	-0.050
H <sub>2</sub> O	4.84	4.84	0.00
<i>Carbons (<sup>13</sup>C NMR in Me<sub>2</sub>SO-d<sub>6</sub>)</i>			
ADM-10			
C-1 + C-3 ( $\beta$ )	32.26	36.18	-0.08
C-2( $\alpha$ )	30.11	30.04	-0.07
C-4 + C-9( $\gamma_{syn}$ )	32.49	32.42	-0.07
C-5( $\delta_{syn}$ )	27.12	28.50	+1.38
C-7( $\delta_{anti}$ )	26.87	26.80	-0.07
C-6( $\epsilon$ )	38.1	38.26	+0.16
CH <sub>3</sub>	14.15	13.98	-0.17
CH <sub>2</sub>	15.53	15.45	-0.08

<sup>a</sup> Only the protons and carbons that show chemical shift changes.

molecules. All three water molecules form additional hydrogen bonds both to other water molecules and to cyclodextrin sugar ring oxygens. Although hydrogen atoms are not modelled for the water molecules, the highest peak in the difference Fourier synthesis (for the low-temperature data) and two more minor Fourier peaks clearly correspond to hydrogen atoms donated by the water molecules to the Br<sup>-</sup> ion.

The tertiary nitrogen is far from the CD cavity and does not show any specific interaction with neighbouring atoms. The C-15 and C-16 atoms, prone to make C-H...O hydrogen bonds, do not show any such interactions.

There is a complex and extended hydrogen

bonding network between the water molecules and the cyclodextrin and ligand. Every water molecule is involved in at least one hydrogen bond mainly with O-2, O-3 and O-6 of the seven sugar moieties comprising the cyclodextrin. All O-2, O-3 and O-6 atoms are involved in a hydrogen bond with at least one water molecule from the same or another asymmetric unit. Only one water molecule hydrogen bonds to the oxygen attached to the adamantane moiety. This water molecule in turn interacts with another water molecule attached to the O-3 atom of one of the monosaccharide rings. This is the only hydrogen bonding interaction between the ligand and the cyclodextrin molecule in which the hydrophobic part of the ligand is buried. The same oxygen atom is

hydrogen bonded to the O-3 atom of the monosaccharide ring of a cyclodextrin molecule related by the  $2_1$  symmetry along the  $a$  axis.

The ADM-10 and  $\beta$ CD atoms show a number of contacts listed in Table 1. Briefly, eleven interactions occur between  $\beta$ CD and the adamantane moiety (nine are H...H interactions and two between the O-4 atoms connecting the saccharide rings and H atoms of the adamantane), whereas four interactions occur between the first part of the tail of ADM-10 and  $\beta$ CD.

Puckering amplitudes, useful indices of the conformation of cyclodextrin saccharide rings, range from 0.553 to 0.592 and are typical for the conformation of  $\beta$ CD rings [6].

*Description of the solution structure.*—The study of complex formation of ADM-10 with  $\beta$ CD in solution was performed by studying  $^1\text{H}$  NMR and  $^{13}\text{C}$  NMR spectra of the free compound (ADM-10) and of the complex.

As a consequence of inclusion, protons attached to C-3 and C-5 of the glucose subunits of  $\beta$ CD, which are located in the interior of the cavity, show an upfield shift ( $\Delta\delta = \delta_{\text{free}} - \delta_{\text{obs}}$ ) of the signals due to a microsolvant effect arising from the ousting of water molecules of the  $\beta$ CD cavity. This effect is more pronounced for the protons at C-5 (Table 2) of the saccharide units. In the case of the ADM-10 molecule, the observed downfield shift changes of the adamantane moiety are in the range 0.07–0.16 ppm (Table 2). At the same time the protons of the polymethylenic chain were not influenced by complex formation, remaining at the same resonance. These chemical shift modifications are indicative of the burying of the bulky adamantane moiety in the cavity.

In the spectrum of the free molecule ADM-10, a triplet at 1.28 ppm corresponds to the terminal methyl group of the linear decanyl part of the molecule, and the multiplet at 1.35 ppm corresponds to the  $(\text{CH}_2)_7$  moiety of the decanyl chain. The undistorted chair conformation of the six membered rings of the rigid adamantane group gives rise to characteristic absorption bands. Thus the broad doublet at 1.57 ppm ( $J$  12 Hz) can be ascribed to the 4 eq and 9 eq protons of the 1,2,3,4,5,9 ring of the

adamantane moiety, and the broad doublet at 2.09 ppm ( $J$  = 12 Hz) to the 4 ax and 9 ax protons of the same ring. All skeletal protons, besides the 4 ax, 4 eq, 9 ax and 9 eq protons, appear as a broad multiplet in which no vicinal coupling constants are detectable [7–9]. The hydrogen atoms of the two methyl groups attached to the nitrogen atom appeared as a sharp singlet at 3.06 ppm. The largest  $\Delta\delta$  values, observed for the 4 ax and 9 ax protons, are in the range of 0.16 ppm. Smaller shift changes are observed in the signals corresponding to the 4 eq and 9 eq protons (0.071 ppm).

The most prominent characteristic of the  $^{13}\text{C}$  NMR experiment is a large positive shift for C-5 of ADM-10, upon formation of the complex of ADM-10 with  $\beta$ CD (Table 2).

*Comparison of crystal and solution structures.*—The most important result from the NMR studies, the burying of the hydrophobic adamantane group inside the  $\beta$ -cyclodextrin molecule, is consistent with the crystallographic results. Most shifts observed by both  $^1\text{H}$  NMR and  $^{13}\text{C}$  NMR spectroscopy can be explained by studying in detail the crystal structure of the complex of ADM-10 with  $\beta$ CD. Nevertheless, the possibility that differences in fine detail exist should not be excluded.

The hydrogen atoms that show the largest chemical shifts in the  $^1\text{H}$  NMR studies upon complex formation, 4 ax and 9 ax (Table 2), face the solvent in the crystal structure (Fig. 4(c)). However, these shifts can be explained based on the interactions observed in the crystal structure (Table 1), which show that one of the closest contacts between ADM-10 and  $\beta$ CD is that between H-4A(4 ax) and H-3 of the Glc<sup>I</sup> saccharide unit of  $\beta$ CD (2.33 Å), a contact sufficient to account for the large change in the doublet.

The C-5 atom of the adamantane moiety, showing a large positive shift in the  $^{13}\text{C}$  NMR spectrum, is close to O-4 connecting the Glc<sup>I</sup> and Glc<sup>II</sup> monosaccharide rings (O-4–C-5 = 3.65 Å). Its proton (H-5, O-4–H-5 = 2.70 Å) might thus be delocalised towards the O-4 atom, resulting in a deprotection of the C-5 atom observed as a positive shift in the  $^{13}\text{C}$  NMR experiment.

The larger shifts for H-5 as compared to H-3 of  $\beta$ CD in the  $^1\text{H}$  NMR experiment cannot be fully understood on the basis of the crystal structure. The number of close contacts observed for H-3 is significantly larger than that for H-5 (Table 1).

The results of this study further signify that X-ray crystallography is an invaluable tool for the study of cyclodextrins complexed with guest molecules. However, it is evident that extrapolation of comparative conclusions of molecular behaviour of potential CD guest molecules, based on the crystal structure alone, should be handled with care.

*Comparison of low- and room-temperature structures.*—Surprisingly, the cell for the low-temperature structure is slightly larger in volume than at room temperature. There are no changes in the  $a$  and  $b$  axes, but a small increase by 0.2 Å in the  $c$  axis. This can probably be attributed to imperfect isomorphism of the crystals, or to changes upon freezing which are related to the ordering of the ADM-10 tail. The ADM-10 tail extends along the  $c$  axis of the cell, and ordering might lead to a slight expulsion of the adjacent cyclodextrin molecule and subsequent lengthening of the axis. In support for the latter hypothesis, the distance between the quaternary nitrogen (start of the disordered tail) and the last carbon (end of the disordered tail) along the  $c$  axis is 8.85 and 9.0 Å in the room-temperature structure (for each conformation) and becomes 9.3 Å in the low-temperature structure, which correlates well with the observed increase along the  $c$ -axis.

The most striking difference in the low-temperature structure is that the disorder of the tail of the ADM-10 molecule is ‘frozen out’ and the tail clearly lies in a single conformation (Fig. 4(a,b)). In addition, two slightly disordered adamantane carbons (C-1, C-3) are more clearly visible in the low-temperature structure. There are no other significant differences.

*Applicability of the X-ray methodology to similar projects.*—The protocol presented hereby for improving initial phase estimates (which can originate both from Patterson and direct methods) and essentially automatically building a complete model, from maps otherwise not interpretable by manual inspection, is

of general applicability. The molecular size of cyclodextrin complexes and the typical diffraction limits for crystals of such complexes, are usually adequate to give ab initio phase estimates; however in some cases initial phases can be of such poor quality that map interpretation can be tedious and time consuming. ARP [10] (as described in Section 3) can generate essentially complete models from noninterpretable maps, provided that initial phase estimates are available and diffraction data extend to a resolution better than 1.2–1.5 Å [11]. As judged after full refinement of the structure, the similarity (real space correlation coefficient) of the starting electron density map to the final refined electron density was only 37% (Fig. 5). The similarity of the map from the ARP procedure to the final refined map was 94%. The ARP package is available as part of the CCP4 [12] package.<sup>1</sup>

Low-temperature data collection, common practice for small molecules and gaining increasing popularity in protein crystallography, in conjunction with synchrotron X-ray radiation, may provide data of very good quality. As synchrotron beam lines increase both in number and intensity, more time will become available for projects such as the study of cyclodextrin complexes. A total of 24 h of synchrotron beam time on a medium-performance beam line can easily provide excellent quality data to atomic resolution for 3–5 such projects. Some scepticism might arise from the belief that cell constants cannot be accurately estimated upon data collection with an image plate scanner. As documented in Refs [13,14], cell constants can indeed be estimated with acceptable accuracy. Furthermore, current beam line calibration procedures with the use of silicon powder diffraction images and least-squares fitting of the observed to calculated pattern<sup>2</sup> can ensure the proper measurement of radiation wavelength and crystal-plate distance and significantly increase the accuracy for cell measurements.

<sup>1</sup> This is available through WWW from: <http://www.embl-hamburg.de/ARP>.

<sup>2</sup> Lamzin and Wilson, to be published.

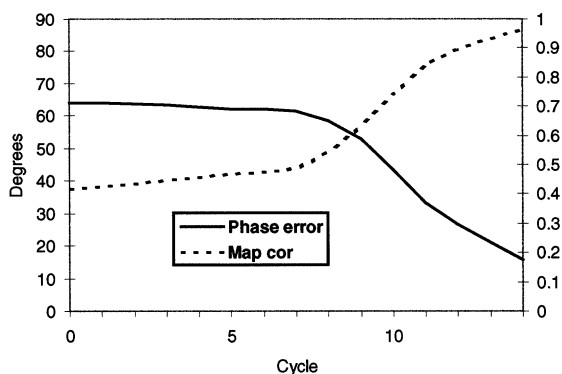


Fig. 5. Phase error and map correlation coefficient as function of ARP refinement cycle.

Table 3

Crystal data and data collection statistics for the room-temperature and cryogenic data

	293 K	150 K
Space group	$P2_12_12_1$	$P2_12_12_1$
$a, b, c$ (Å)	15.486, 17.016, 32.009	15.483, 17.053, 32.231
Estimated std in cell dimensions	0.027, 0.042, 0.040	0.019, 0.020, 0.044
Volume (Å <sup>3</sup> )	8434.7	8510.1
Wavelength (Å)	0.750	0.870
Maximum resolution (Å)	1.03	0.90
Reflections measured	27142	52927
Reflections expected	7706	11640
Unique reflections	7463	11398
Redundancy	3.6	4.6
Completeness (%) ( <i>high resol. shell</i> )	95.2 (80.1)	95.2 (82.8)
$R_{\text{sym}}^a$ (%) ( <i>high resol. shell</i> )	8.4 (27.6)	8.6 (21.1)
$I/\sigma(I)$ ( <i>high resol. shell</i> )	9.4 (2.4)	12.0 (4.1)
$R(\sigma)^b$ (%)	9.8	9.6

$$^a R_{\text{sym}} = \frac{\sum |I - \langle I \rangle|}{\sum I}$$

$$^b R(\sigma) = \frac{\sum \sigma(I)}{\sum I}$$

### 3. Experimental

**Crystallisation and X-ray data collection.**—The bromide salt of 2-(3-dimethylamino-propyl)tricyclo[3.3.1.1<sup>3,7</sup>]decan-2-ol (ADM-10) was dissolved in water, together with  $\beta$ -cyclodextrin, and crystallised by slow evaporation from distilled water. The crystals used for data collection were needles of approximate dimensions  $0.02 \times 0.02 \times 0.1$  mm. They belong to the orthorhombic space group  $P2_12_12_1$  with cell dimensions  $15.5 \times 17.0 \times 32.0$  Å.

For room-temperature data, the crystals were glued at the end of a glass fibre. Synchrotron radiation was used on the EMBL X31 beamline at DESY, Hamburg, with a wavelength of 0.75 Å to maximise the anomalous scattering of the Br<sup>-</sup> ion. The rotation method [15] was employed, which is mainly used in protein crystallography but can also provide accurate data for small molecule structures [13]. A MAR image plate area detector was used. Data were collected to a resolution of 1.15 Å, within 3 h. Images were indexed and scaled with the programs DENZO and SCALEPACK [16]. The cell was estimated from a post-refinement procedure as described in Ref. [14]. After merging of multiple recorded and symmetry equivalent reflections, the overall reliability index  $R_{\text{sym}}$  was 8.3% (Table 3).

For low-temperature data, the crystals were transferred to a drop of perfluorinated ether [17] and picked up with a small loop of wool fibre, with approximate diameter of 1 mm. They were subsequently exposed to a stream of evaporating N<sub>2</sub> at 150 K [18]. Data were collected on the BW7 EMBL beamline. Use of a bigger image plate (in comparison with the room-temperature data) allowed the collection of data to a maximum resolution of 0.9 Å.  $R_{\text{sym}}$  for these data was 5.8% (Table 3).

**Crystal structure solution.**—The structure was solved using the room-temperature data. The position of the Br<sup>-</sup> ion was located from both the Patterson synthesis and the anomalous difference Patterson synthesis, utilising the program SHELXS86 [19]. Attempts to get a good-quality map using either Patterson expansion methods or direct methods were unsuccessful.

A novel protocol was applied to obtain an interpretable map. The program suite ARP [10] (used in protein crystallography for improvement and completion of atomic models) was used. Here on, we describe the protocol, not as it was originally used, but after optimisation:

The single Br<sup>-</sup> ion located from the native Patterson synthesis was used as an initial model. Starting from this atom, a model consisting of only O atoms was slowly created by

ARP. ARP is a cyclic procedure, consisting of two parts: (1) unrestrained maximum likelihood minimization in reciprocal space, to properly match calculated to observed structure factor amplitudes and (2) substantial modification of the current atomic dummy model in real space. For the unrestrained refinement step, the REFMAC program [20] from the CCP4 suite was used. ARP, after each reciprocal space refinement cycle, updated the model, mimicking human intervention between refinement cycles. Atoms were removed based on the density in the  $3F_o - 2F_c$  Fourier synthesis (if the density at an atomic center was below 1.4 rms density) and added in significant density in the  $F_o - F_c$  Fourier synthesis (if the density was higher than 3.5 rms and provided that they were bonded to existing atoms). In the initial three cycles, where the model was highly incomplete, only one atom was allowed to be added and no atoms were removed. In these initial cycles, no interatomic vectors parallel to a crystallographic axis were allowed during atoms addition, to avoid interpreting the expected noise along the  $b$  axis (because the  $\text{Br}^-$  ion was approximately at position  $x, 0.5, z$ ) as atomic positions. Addition of these first atoms defines the enantiomer and it is by pure chance that in this case the correct enantiomer was chosen. An additional 12 cycles, where 15 atoms were allowed to be removed or added, were adequate for convergence of ARP and resulted in an excellent map (Fig. 5). It must be noted that the program automatically decides to avoid certain interatomic vectors and estimates the number of atoms to add or remove on the basis of model completeness. The total procedure of ARP refinement takes  $\sim 30$  min on a Silicon Graphics Indy R4400/200 MHz workstation. At the end, all non-H atoms of the cyclodextrin, the ligand and ten water molecules were located. Four additional atoms were placed (wrongly) into density: two near the  $\text{Br}^-$  ion (accounting for the anisotropic displacement of the ion which at that stage was obviously refined isotropically) and two to hydrogen positions.

*Refinement of the crystal structure.*—After identifying and assigning the correct atom types, the model was subjected to ten cycles of

full matrix least-squares refinement using SHELXL-93 [21]. Restrained anisotropic displacement parameters (DELU and SIMU) were employed for all non-H atoms. Restraints forcing the sugar moieties of the cyclodextrin to have similar geometries were used. Hydrogen atoms were added and an additional 20 cycles of refinement were performed in which each non-hydrogen atom was assigned an anisotropic temperature factor. As judged by manual inspection of the  $3F_o - 2F_c$  Fourier maps using the program o [22], the tail was disordered and after C-21 (Fig. 2) it adopted two alternative conformations. These conformations were successfully modelled and refined with varying occupancies, whose sum was restricted to unity. The relative occupancies of these two conformations were found to be 55 and 45%. After adjustment of the weighting scheme the final  $R$  factor converged to 7.6% (Table 4).

For the low-temperature data, the H atoms and anisotropic temperature factors of the room-temperature model were removed together with the double conformation for the tail and the model was subjected to ten cycles

Table 4  
Refinement statistics for the room-temperature and cryogenic data

	293 K	150 K
Reflections used	7573	11733
Parameters	1096	1041
Restraints	1778	1598
Weight <sup>a</sup> A	0.1029	0.0779
Weight B	11.3713	10.6274
$wR_2$ <sup>b</sup> (%)	19.4	17.8
$R_1$ <sup>c</sup> (%)	8.7	7.1
$R_1 (F_o > 4\sigma F_o)$ (%)	7.2	6.4
GOF <sup>d</sup>	1.18	1.05
Restrained GOF	1.08	0.99

<sup>a</sup> Weight =  $1/\sigma^2 (F_o^2) + (\text{Weight A} \times P)^2 + \text{Weight B} \times P$ , where  $P = (F_o^2 + 2F_c^2)/3$ ;

<sup>b</sup>  $wR_2 = \Sigma w(F_o^2 - F_c^2)^2 / \Sigma w(F_o^2)^2$ ;

<sup>c</sup>  $R_1 = \Sigma ||F_o| - |F_c|| / \Sigma |F_o|$ ;

<sup>d</sup> GOF =  $\Sigma w(F_o^2 - F_c^2)^2 / (n - p)^2$ , where  $n$  is the number of reflections and  $p$  is the total number of parameters. In the restrained GOF,  $\Sigma w(yt - y)^2$  (where  $y$  is the quantity being restrained and  $yt$  is its target value) is added to the numerator, and the number of restraints is added to the denominator.

of refinement. A similar protocol as for room-temperature data was applied. Inspection of the maps did not show an alternative conformation for the tail, which is 100% in a conformation very close to the major (55%) conformation of the tail at room temperature. The final *R* factor converged to 6.4% (Table 4).

*Nuclear magnetic resonance spectroscopy.*—<sup>1</sup>H NMR spectra were recorded at 200 MHz on a Bruker AC 200 instrument using D<sub>2</sub>O as solvent and tetramethylsilane (Me<sub>4</sub>Si) as external reference. Typical conditions were 16K data points with zero fitting sweep width 1.4 kHz, giving a digital resolution of 0.34 Hz/point acquisition time 2.9 s. Gaussian enhancement was used for the displayed spectra (GB 0.2; LB –2). <sup>13</sup>C NMR spectra were recorded at 50 MHz on the same instrument using Me<sub>2</sub>SO-*d*<sub>6</sub> as solvent and Me<sub>4</sub>Si as external reference. Typical conditions were 32K data points, acquisition time 2.9 s. Lorentzian enhancement was used for the displayed spectra (LB 3).

## References

- [1] J. Szejtli, *Cyclodextrin Technology*, Kluwer, Academic Publishers (1989).
- [2] W. Saenger, *Angew. Chem., Int. Ed. Engl.*, 19 (1980) 344–362.
- [3] W. Saenger, *Isr. J. Chem.*, 25 (1985) 43–50.
- [4] P. Tsitsa, D.A. Berghe, *Eur. J. Med. Chem.*, 28 (1993) 149–158.
- [5] S.C. Harvey, in A.G. Gilman, L.S. Goodman, A. Gilman (Eds.), *Goodman and Gilman's The Pharmacological Basis of Therapeutics*, 6th ed., Macmillan, New York, 1980, pp. 978–979.
- [6] D. Cremer, J.A. Pople, *J. Am. Chem. Soc.*, 97 (1975) 1354–1358.
- [7] Z. Hajek, P. Vodicka, Z. Ksandr, S. Landa, *Tetrahedron Lett.*, 40 (1972) 4103–4106.
- [8] F.W. van Deursen, P.K. Korver, *Tetrahedron Lett.*, 40 (1967) 3923–3928.
- [9] F.W. van Deursen, J. Bakker, *Tetrahedron*, 27 (1971) 4593–4600.
- [10] V.L. Lamzin, K.S. Wilson, *Acta Crystallogr.*, D50 (1993) 129–147.
- [11] A. Perrakis, T.K. Sixma, K.S. Wilson, V.S. Lamzin (1997) in *Recent advances in phasing*, Proceedings of Daresbury study weekend.
- [12] CCP4 *Acta Crystallogr.*, D50 (1994) 760–763.
- [13] J. Grochowski, P. Serda, K.S. Wilson, Z. Dauter, *J. Appl. Cryst.*, 22 (1994) 722–726.
- [14] A. Perrakis, T. Schneider, E. Antoniadou-Vyzas, Z. Dauter, S.J. Hamodrakas, *J. Appl. Cryst.*, 29 (1996) 261–264.
- [15] A. Arndt, A.J. Wonacott, *The Rotation Method in Crystallography*, North Holland Publishing Company, Amsterdam, 1977, pp. 75–103.
- [16] Z. Otwinowski, DENZO: An oscillation data processing program for macromolecular crystallography, Yale University, New Haven, USA, 1993.
- [17] D. Kottke, D. Stalke, *J. Appl. Cryst.*, 26 (1993) 615–619.
- [18] J. Cosier, A.M. Glazer, *J. Appl. Cryst.*, (1986) 105–107.
- [19] G.M. Sheldrick, Shelxs-86, Program for the solution of Crystal Structures. Univ. of Gottingen, Germany, 1985.
- [20] G. Murshudov, A. Vagin, E. Dodson, (1996) Application of maximum likelihood refinement, in *The refinement of protein structures*, Proceedings of Daresbury study weekend.
- [21] G.M. Sheldrick, Shelxl-93, Program for Crystal Structure refinement. Univ. of Gottingen, Germany, 1993.
- [22] A. Jones, *Acta Crystallogr.*, A47 (1991) 110–119.
- [23] A.L. Spek, PLATON-92, Univ. of Utrecht, The Netherlands, 1992.
- [24] P.J. Kraulis, *J. Appl. Cryst.*, 24 (1996) 946–950.